US012387392B2

(12) **United States Patent**
Wang et al.

(10) **Patent No.: US 12,387,392 B2**
(45) **Date of Patent: Aug. 12, 2025**

(54) **HYBRID IMAGE RECONSTRUCTION SYSTEM**

(71) Applicant: **Rensselaer Polytechnic Institute**, Troy, NY (US)

(72) Inventors: **Ge Wang**, Loudonville, NY (US); **Weiwen Wu**, Troy, NY (US); **Wenxiang Cong**, Albany, NY (US); **Hengyong Yu**, Westford, MA (US)

(73) Assignee: **Rensselaer Polytechnic Institute**, Troy, NY (US)

(*) Notice: Subject to any disclaimer, the term of this patent is extended or adjusted under 35 U.S.C. 154(b) by 710 days.

(21) Appl. No.: **17/393,922**

(22) Filed: **Aug. 4, 2021**

(65) **Prior Publication Data**

US 2022/0044452 A1 Feb. 10, 2022

Related U.S. Application Data

(60) Provisional application No. 63/167,079, filed on Mar. 28, 2021, provisional application No. 63/060,866, filed on Aug. 4, 2020.

(51) **Int. Cl.**
G06T 11/00 (2006.01)
G06N 3/04 (2023.01)
G06N 3/08 (2023.01)

(52) **U.S. Cl.**
CPC ***G06T 11/005*** (2013.01); ***G06N 3/04*** (2013.01); ***G06N 3/08*** (2013.01); *G06T 2210/41* (2013.01)

(58) **Field of Classification Search**
CPC G06T 2210/41; G06T 2207/10076; G06T 11/008; G06T 2207/10072;
(Continued)

(56) **References Cited**

U.S. PATENT DOCUMENTS

6,577,700 B1 * 6/2003 Fan G01N 27/24 378/4
9,305,379 B2 * 4/2016 Stayman G06T 7/38
(Continued)

FOREIGN PATENT DOCUMENTS

EP 3825712 A1 * 5/2021 ..... A61B 5/055
WO WO-2017223560 A1 * 12/2017 ..... A61B 5/00
(Continued)

OTHER PUBLICATIONS

Morteza Mardani et al., "Deep Generative Adversarial Neural Networks for Compressive Sensing MRI", Jan. 2019, IEEE Transactions on Medical Imaging, vol. 38, No. 1, Jan. 2019. (Year: 2019).*

(Continued)

Primary Examiner — Manav Seth
(74) *Attorney, Agent, or Firm* — Barclay Damon LLP; Anthony P. Gangemi

(57) **ABSTRACT**

Generally, there is provided a hybrid image reconstruction system. The hybrid image reconstruction system includes a deep learning stage and a compressed sensing stage. The deep learning stage is configured to receive an input data set that includes measured tomographic data and to produce a deep learning stage output. The deep learning stage includes a mapping circuitry, and at least one artificial neural network. The mapping circuitry is configured to map image domain data to a tomographic data domain. The compressed sensing stage is configured to receive the deep learning stage output and to provide refined image data as output.

23 Claims, 4 Drawing Sheets

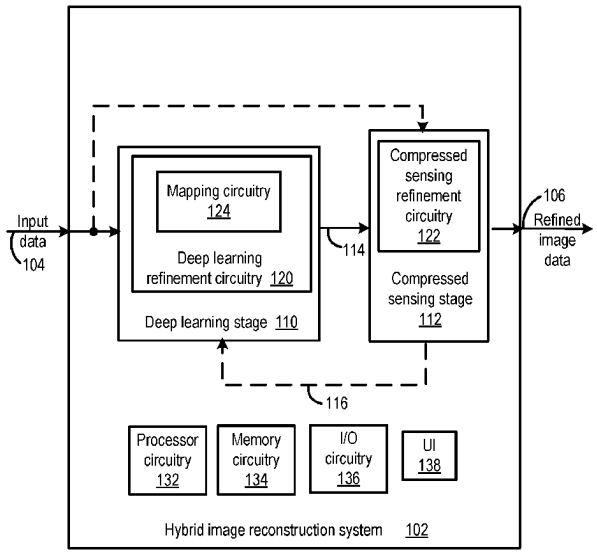

(58) **Field of Classification Search**
CPC . G06T 2207/30004; G06T 2207/10104; G06T 2207/10108; G06T 11/005; G06T 5/00; G06T 2211/441; G06T 2211/436; G06T 2211/424; G06T 2207/20081; G06T 2207/20084; A61B 6/032; A61B 6/5205; A61B 6/52; G06F 18/253; G06F 18/214–2155; G06F 7/023; G06F 40/16; G06N 3/04; G06N 3/08; G06N 3/088; G06N 3/094; G06N 3/02–126; G06N 20/00–20; G06K 9/6256; G06K 9/6257; G06K 9/6259; G06V 10/70; G06V 10/82; G06V 10/774–7796
See application file for complete search history.

(56) **References Cited**

U.S. PATENT DOCUMENTS

10,002,447	B1	6/2018	Cao	
10,049,446	B2	8/2018	Simon	
10,055,861	B2	8/2018	Dempsey	
10,140,734	B2	11/2018	Chen	
10,475,214	B2	11/2019	Fu	
10,607,378	B2	3/2020	Jarisch	
10,628,973	B2	4/2020	De Man	
10,970,887	B2 *	4/2021	Wang	A61B 5/00
11,454,690	B2 *	9/2022	Wang	G01R 33/543
2011/0142316	A1 *	6/2011	Wang	G06T 11/006 382/131
2016/0012615	A1 *	1/2016	Gao	G06T 11/005 382/131
2016/0117850	A1 *	4/2016	Jin	A61B 6/03 382/131
2016/0339381	A1	11/2016	Flaßpohler et al.	
2018/0197317	A1	7/2018	Cheng et al.	
2019/0012814	A1	1/2019	Dempsey et al.	
2019/0251713	A1	8/2019	Chen et al.	
2019/0325621	A1 *	10/2019	Wang	G06N 3/045
2019/0328348	A1	10/2019	De Man et al.	
2019/0378311	A1	12/2019	Mailhe et al.	
2020/0043204	A1	2/2020	Fu et al.	
2020/0090385	A1	3/2020	Jarisch	
2021/0118200	A1 *	4/2021	Akcakaya	G06N 3/08

FOREIGN PATENT DOCUMENTS

WO	WO-2018232388 A1 *	12/2018	A61B 5/7267
WO	WO-2020163783 A1 *	8/2020	A61B 5/00

OTHER PUBLICATIONS

Maximilian Seitzer et al., "Adversarial and Perceptual Refinement for Compressed Sensing MRI Reconstruction", Jun. 28, 2018, https://arxiv.org/abs/1806.11216. (Year: 2018).*
Weiwen Wu et al., "Stabilizing Deep Tomographic Reconstruction Networks", Aug. 4, 2020, https://arxiv.org/abs/2008.01846v1. (Year: 2020).*
Li et al., 2011, "A compressed sensing-based iterative algorithm for CT reconstruction and its possible application to phase contrast imaging" (pp. 1-14) (Year: 2011).*
Sidky et al.; "Do CNNs solve the CT inverse problem?", May 21, 2020; 12 pages.

* cited by examiner

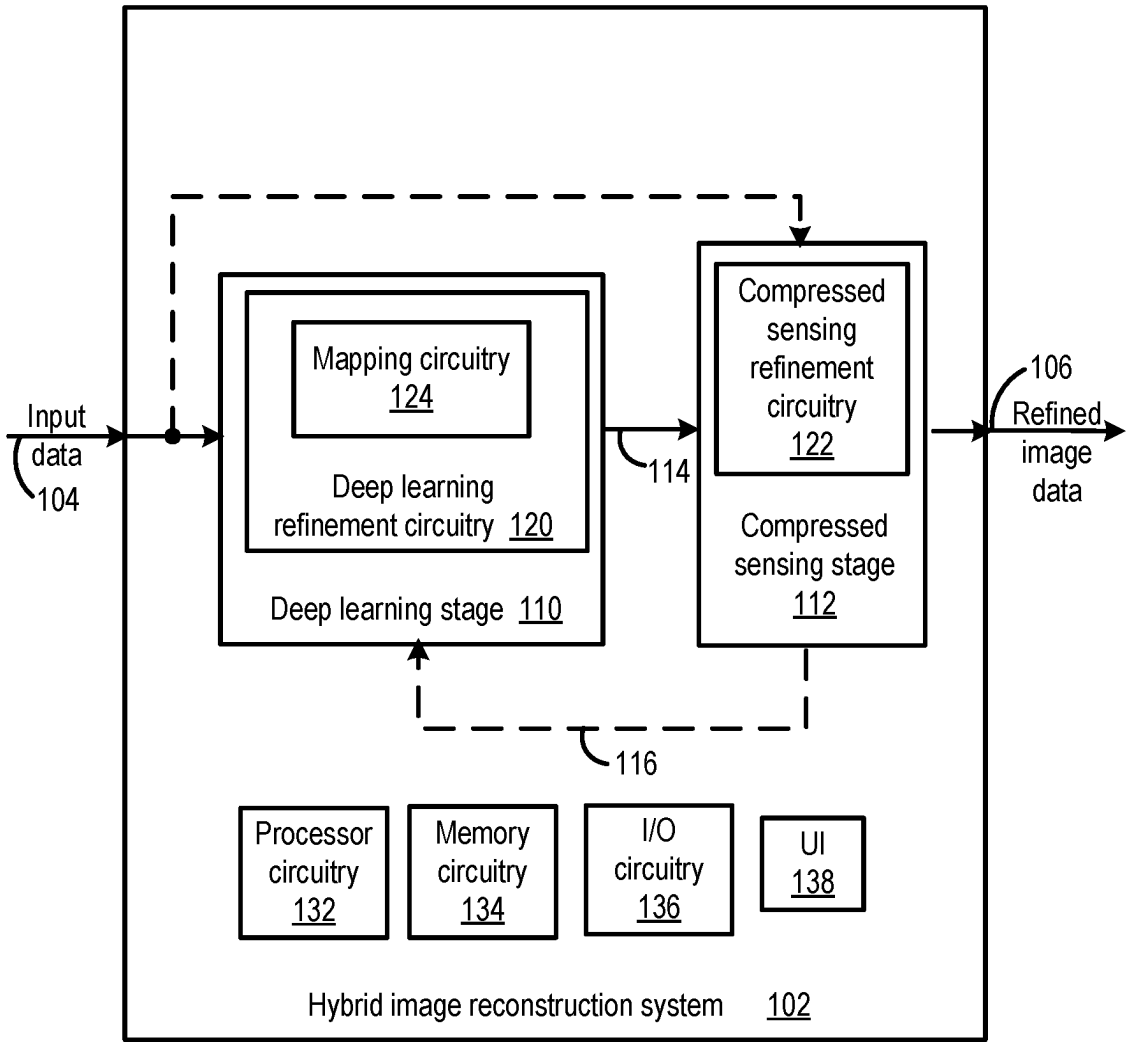
Input data 104
Mapping circuitry 124
Deep learning refinement circuitry 120
Deep learning stage 110
114
Compressed sensing refinement circuitry 122
Compressed sensing stage 112
106
Refined image data
116
Processor circuitry 132
Memory circuitry 134
I/O circuitry 136
UI 138
Hybrid image reconstruction system 102

FIG. 1

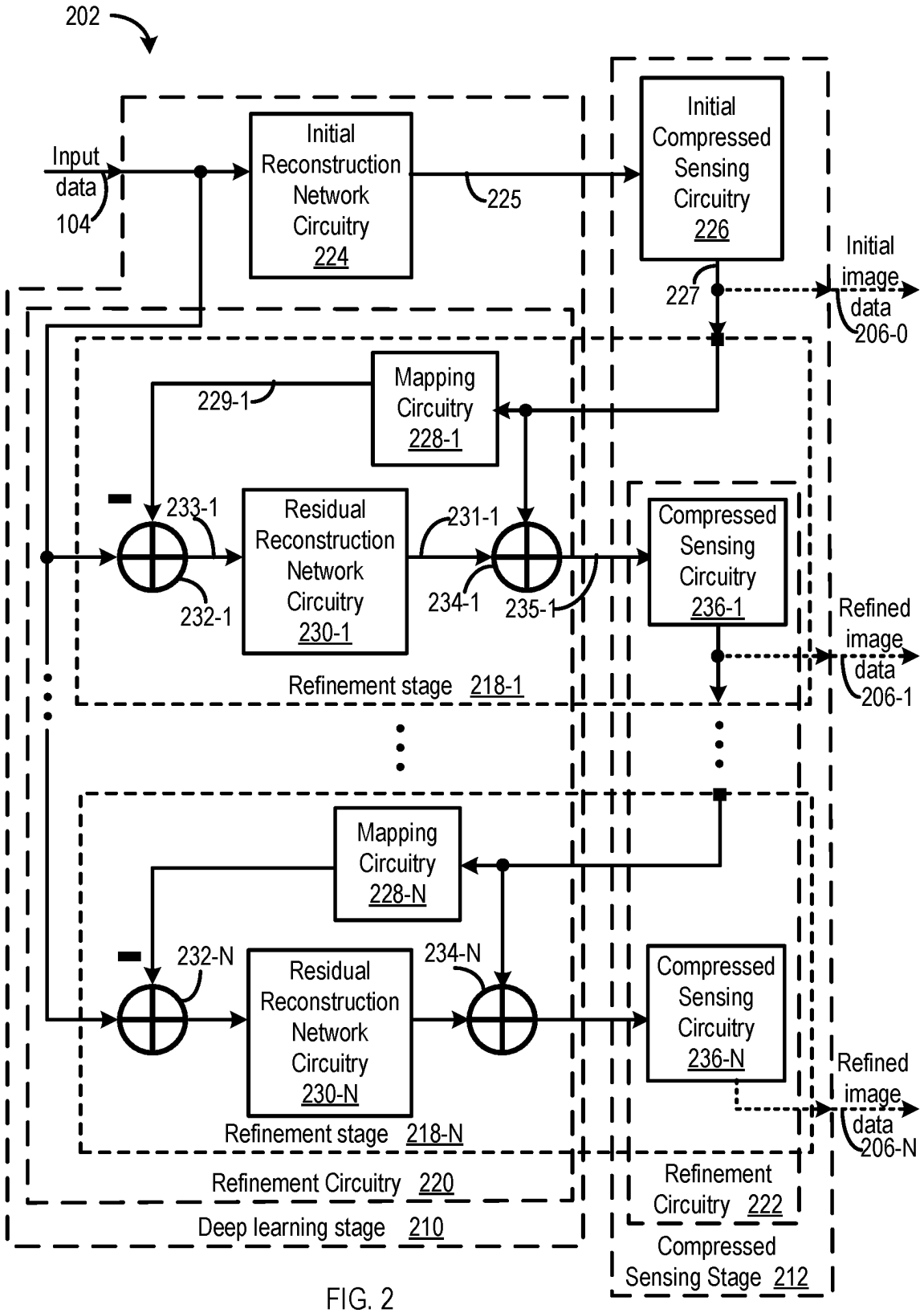
202
Input data 104
Initial Reconstruction Network Circuitry 224
225
Initial Compressed Sensing Circuitry 226
227
Initial image data 206-0
Mapping Circuitry 228-1
229-1
233-1
232-1
Residual Reconstruction Network Circuitry 230-1
231-1
234-1
235-1
Compressed Sensing Circuitry 236-1
Refined image data 206-1
Refinement stage 218-1
Mapping Circuitry 228-N
232-N
234-N
Residual Reconstruction Network Circuitry 230-N
Compressed Sensing Circuitry 236-N
Refined image data 206-N
Refinement stage 218-N
Refinement Circuitry 220
Deep learning stage 210
Refinement Circuitry 222
Compressed Sensing Stage 212

FIG. 2

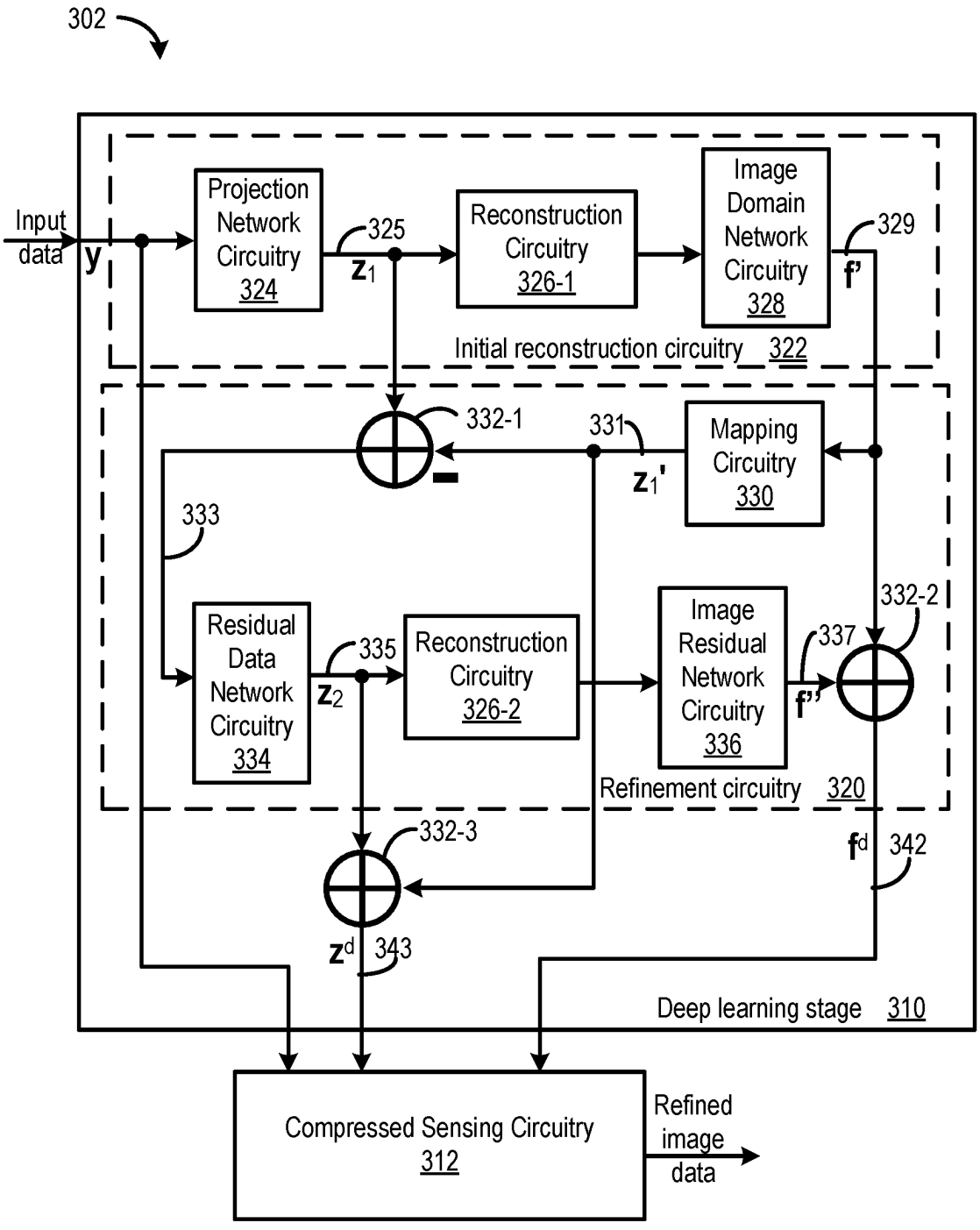
302
Input data
y
Projection Network Circuitry 324
325
z1
Reconstruction Circuitry 326-1
Image Domain Network Circuitry 328
329
f'
Initial reconstruction circuitry 322
332-1
331
z1'
Mapping Circuitry 330
333
Residual Data Network Circuitry 334
335
z2
Reconstruction Circuitry 326-2
Image Residual Network Circuitry 336
337
f''
332-2
Refinement circuitry 320
332-3
fd
342
zd
343
Deep learning stage 310
Compressed Sensing Circuitry 312
Refined image data

FIG. 3

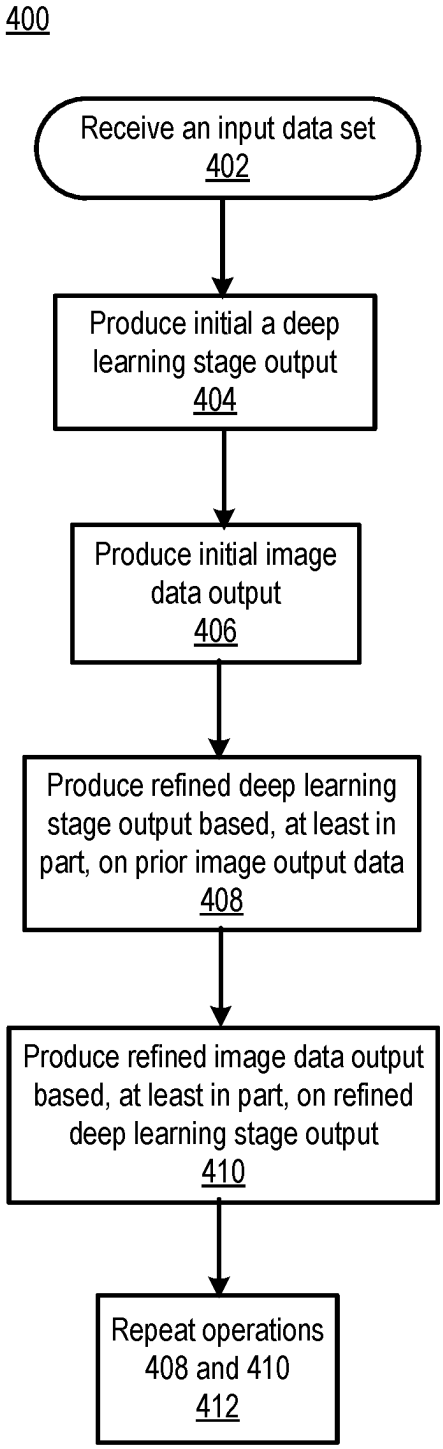
400
Receive an input data set
402
Produce initial a deep learning stage output
404
Produce initial image data output
406
Produce refined deep learning stage output based, at least in part, on prior image output data
408
Produce refined image data output based, at least in part, on refined deep learning stage output
410
Repeat operations 408 and 410
412

FIG. 4

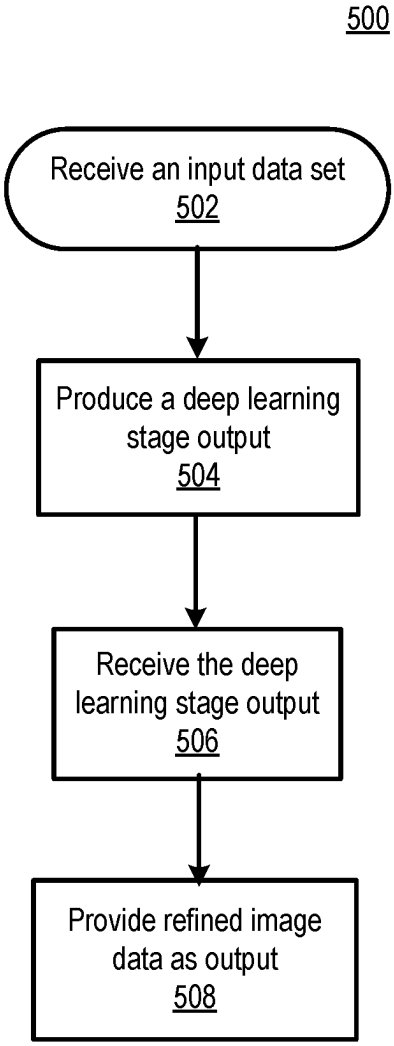
500
Receive an input data set
502
Produce a deep learning stage output
504
Receive the deep learning stage output
506
Provide refined image data as output
508

FIG. 5

HYBRID IMAGE RECONSTRUCTION SYSTEM

CROSS REFERENCE TO RELATED APPLICATION(S)

This application claims the benefit of U.S. Provisional Application No. 63/060,866, filed Aug. 4, 2020, and U.S. Provisional Application No. 63/167,079, filed Mar. 28, 2021, which are incorporated by reference as if disclosed herein in their entireties.

GOVERNMENT LICENSE RIGHTS

This invention was made with government support under award numbers EB017140, CA237267, CA233888, and EB026646, awarded by the National Institutes of Health. The government has certain rights in the invention.

FIELD

The present disclosure is related to a reconstruction system, in particular to, a hybrid image reconstruction system.

BACKGROUND

Tomographic image reconstruction with deep learning (DL) is an emerging field of applied artificial intelligence. At least some deep reconstruction networks may be unstable such as for computed tomography (CT) and magnetic resonance imaging (MRI). Instabilities may include, for example, strong output artefacts from tiny perturbation, small features being undetectable, and increased input data degrading performance. Such instabilities may be contrasted to sparsity-regularized reconstruction methods that do not suffer from these instabilities, due, at least in part, to kernel awareness. Since deep reconstruction is a mainstream approach to achieve better tomographic image quality, there is a need for stabilizing deep tomographic reconstruction networks.

Deep learning has attracted attention in the field of tomographic image reconstruction, including, for example, CT, MM, positron emission tomography/single photon emission computed tomography (PET/SPECT), ultrasound and optical imaging. Sparse-view CT, in particular, remains a challenge that targets an acceptable image reconstruction from ultra-sparse projections.

SUMMARY

In some embodiments, there is provided a hybrid image reconstruction system. The hybrid image reconstruction system includes a deep learning stage and a compressed sensing stage. The deep learning stage is configured to receive an input data set that includes measured tomographic data and to produce a deep learning stage output. The deep learning stage includes a mapping circuitry, and at least one artificial neural network. The mapping circuitry is configured to map image domain data to a tomographic data domain. The compressed sensing stage is configured to receive the deep learning stage output and to provide refined image data as output.

In some embodiments of the hybrid image reconstruction system, the deep learning stage includes an initial reconstruction network circuitry, and a deep learning stage refinement circuitry including at least one mapping circuitry, and at least one residual reconstruction network circuitry. The compressed sensing stage includes an initial compressed sensing circuitry, and a compressed sensing stage refinement circuitry including at least one refinement compressed sensing circuitry. At least a portion of the deep learning stage refinement circuitry and at least a portion of the compressed sensing stage refinement circuitry correspond to a refinement stage. The initial reconstruction network circuitry is configured to receive the input data set and to reconstruct a corresponding initial image data. The initial compressed sensing circuitry is configured to regularize the initial image data to yield an estimated image data. Each mapping circuitry is configured to receive a prior compressed sensing circuitry image data output and to produce a respective corresponding projection data set. Each residual reconstruction network circuitry is configured to receive a respective residual projection data set corresponding to a difference between the input data set and the respective prior corresponding projection data set and to determine a respective corresponding residual image data. Each refinement compressed sensing circuitry is configured to receive a sum of a prior compressed sensing circuitry image data output and the respective corresponding residual image data and to produce a respective refined image data output.

In some embodiments of the hybrid image reconstruction system, a system architecture corresponds to an unrolled network architecture that comprises a plurality of refinement stages.

In some embodiments of the hybrid image reconstruction system, a respective refinement stage includes a respective mapping circuitry, a respective residual reconstruction circuitry and a respective refinement compressed sensing circuitry.

In some embodiments of the hybrid image reconstruction system, each residual projection data set is normalized and each residual image data is denormalized.

In some embodiments of the hybrid image reconstruction system, the deep learning stage includes an initial reconstruction circuitry, and a refinement circuitry. The initial reconstruction circuitry is configured to receive the input data set, to determine an estimated projection data set based, at least in part, on the input data set, and to determine an refined image data set based, at least in part, on the estimated projection data set. The refinement circuitry is configured to receive the estimated projection data set and the refined image domain data set, and to determine an updated data—image pair. The updated data—image pair corresponds to the deep learning stage output.

In some embodiments of the hybrid image reconstruction system, the initial reconstruction circuitry includes a projection network circuitry, and an image domain network circuitry. The refinement circuitry includes a residual data network circuitry, and an image residual network circuitry. Each network circuitry corresponds to an artificial neural network configured to operate in a projection data domain or an image data domain.

In some embodiments of the hybrid image reconstruction system, the input data set is sparse and the estimated measurements are relatively highly dimensional.

In some embodiments of the hybrid image reconstruction system, the projection network circuitry and the image domain network circuitry each corresponds to a respective encode-decode network and the image domain network circuitry corresponds to a generative adversarial network (GAN).

In some embodiments of the hybrid image reconstruction system, the input data is selected from the group including

computed tomography (CT), magnetic resonance imaging (MRI), positron emission tomography (PET), and single photon emission computed tomography (SPECT) tomographic data.

In an embodiment, there is provided a method for hybrid image reconstruction. The method includes receiving, by a deep learning stage, an input data set comprising measured tomographic data; and producing, by the deep learning stage, a deep learning stage output. The deep learning stage includes a mapping circuitry, and at least one artificial neural network. The mapping circuitry is configured to map image domain data to a tomographic data domain. The method further includes receiving, by a compressed sensing stage, the deep learning stage output; and providing, by the compressed sensing stage, refined image data as output.

In some embodiments of the method, the deep learning stage includes an initial reconstruction network circuitry, and a deep learning stage refinement circuitry comprising at least one mapping circuitry, and at least one residual reconstruction network circuitry, and the compressed sensing stage comprises an initial compressed sensing circuitry, and a compressed sensing stage refinement circuitry comprising at least one refinement compressed sensing circuitry, at least a portion of the deep learning stage refinement circuitry and at least a portion of the compressed sensing stage refinement circuitry corresponding to a refinement stage. The method further includes reconstructing, by the initial reconstruction network circuitry, a corresponding initial image data based, at least in part, on the input data set; and regularizing, by the initial compressed sensing circuitry, the initial image data to yield an estimated image data. The method further includes producing, by each mapping circuitry, a respective corresponding projection data set based, at least in part on, a prior compressed sensing circuitry image data output; producing, by each residual reconstruction network circuitry, a respective corresponding residual image data based, at least in part, on a respective residual projection data set corresponding to a difference between the input data set and the respective prior corresponding projection data set; receiving, by each refinement compressed sensing circuitry, a sum of a prior compressed sensing circuitry image data output and the respective corresponding residual image data; and producing, by each refinement compressed sensing circuitry, a respective refined image data output.

In some embodiments of the method, a system architecture corresponds to an unrolled network architecture that comprises a plurality of refinement stages.

In some embodiments of the method, a respective refinement stage includes a respective mapping circuitry, a respective residual reconstruction circuitry and a respective refinement compressed sensing circuitry.

In some embodiments of the method, each residual projection data set is normalized and each residual image data is denormalized.

In some embodiments of the method, the deep learning stage includes an initial reconstruction circuitry, and a refinement circuitry. The method further includes receiving, by the initial reconstruction circuitry, the input data set; determining, by the initial reconstruction circuitry, an estimated projection data set based, at least in part, on the input data set; determining, by the initial reconstruction circuitry, an refined image data set based, at least in part, on the estimated projection data set. The method further includes receiving, by the refinement circuitry, the estimated projection data set and the refined image domain data set; and determining, by the refinement circuitry, an updated data—image pair. The updated data—image pair corresponds to the deep learning stage output.

In some embodiments of the method, the initial reconstruction circuitry includes a projection network circuitry, and an image domain network circuitry. The refinement circuitry includes a residual data network circuitry, and an image residual network circuitry. Each network circuitry corresponds to an artificial neural network configured to operate in a projection data domain or an image data domain.

In some embodiments of the method, the input data set is sparse and the estimated measurements are relatively highly dimensional.

In some embodiments of the method, the projection network circuitry and the image domain network circuitry each corresponds to a respective encode-decode network and the image domain network circuitry corresponds to a generative adversarial network (GAN).

In some embodiments of the method, the input data is selected from the group including computed tomography (CT), magnetic resonance imaging (MM), positron emission tomography (PET), and single photon emission computed tomography (SPECT) input data.

In some embodiments, a computer readable storage device having stored thereon instructions that when executed by one or more processors result in the following operations including any one of the embodiments of the method.

BRIEF DESCRIPTION OF THE DRAWINGS

The drawings show embodiments of the disclosed subject matter for the purpose of illustrating features and advantages of the disclosed subject matter. However, it should be understood that the present application is not limited to the precise arrangements and instrumentalities shown in the drawings, wherein:

FIG. **1** illustrates a functional block diagram of a hybrid image reconstruction system consistent with several embodiments of the present disclosure;

FIG. **2** illustrates a functional block diagram of one embodiment of a hybrid image reconstruction system according to the present disclosure;

FIG. **3** illustrates a functional block diagram of another embodiment of a hybrid image reconstruction system according to the present disclosure;

FIG. **4** is a flowchart of example hybrid image reconstruction operations consistent with various embodiments of the present disclosure; and

FIG. **5** is a flowchart of another example hybrid image reconstruction operations consistent with various embodiments of the present disclosure.

DETAILED DESCRIPTION

Generally, this disclosure relates to a hybrid image reconstruction system. In some embodiments, the hybrid image reconstruction system includes a deep learning stage and a compressed sensing stage. The deep learning stage is configured to receive an input data set that includes measured tomographic data and to produce a deep learning stage output. The deep learning stage includes a mapping circuitry, and at least one artificial neural network. The mapping circuitry is configured to map image domain data to a tomographic data domain. The compressed sensing stage is

configured to receive the deep learning stage output and to provide refined image data as output.

In one embodiment, the hybrid image reconstruction system may correspond to an analytic compressive iterative deep framework ("ACID"). In another embodiment, the hybrid image reconstruction system may correspond to a dual-domain residual-based optimization network (DRONE). A deep reconstruction network may be stabilized in a hybrid model that combines deep learning and compressed sensing.

Turning first to the ACID embodiment, given a deep reconstruction network and measurement data (i.e., input data), an image can first be reconstructed by the reconstruction network but the reconstruction may compromise fine details and/or introduce artifacts. A compressed sensing inspired module may be used to enforce sparsity in the image domain, with a loss function configured to capture both data fidelity and sparsity (e.g., total variation (TV), low-rank, dictionary learning, etc.). A forward imaging model may be configured to project an intermediate reconstructed image to a raw data domain to estimate tomographic data. It may be appreciated that estimated tomographic data may be generally differ from the original data. The difference is a data residual that may not be explained by the current image. From the data residual, an incremental image may be reconstructed with the reconstruction network to update the current image through the reconstruction network. The process may be repeated to prevent losing or falsifying features. ACID may thus generally include three modules: deep reconstruction for data-driven priors ("deep"), compressed sensing inspired sparsity promotion ("compressive"), and analytic mapping to estimate data ("analytic"). Workflow through the three modules may be iterative, cycling through these three modules providing a solution in an intersection of the space of data-driven solutions, the space of sparse solutions, and the space of solutions subject to data constraints.

It may be appreciated that stability of a hybrid image reconstruction system may be related to convergence. For example, stability may be related to convergence of an ACID iterative workflow. A bounded error norm (BEN) property of a proper reconstruction network, as characterized by a ratio being less than 1 between a norm of a reconstruction error and a norm of a corresponding ground truth; that is, the error component of the initial image reconstructed by a deep network, e.g., reconstruction network circuitry of FIG. **2**, as described herein, is less than a ground truth image in an L2 norm sense. The error includes two components: sparse and non-sparse. The non-sparse component may then be effectively suppressed by a compressive sensing (CS) inspired sparsity promotion module, e.g., compressed sensing circuitry of FIG. **2**.

The sparse errors are either observable or unobservable. The unobservable error is in the null space of the system matrix A (e.g., mapping circuitry of FIG. **2**), and should be small relative to the null space component of the ground truth image because a proper reconstruction network is intended to recover the null space component well in a data-driven fashion. ACID may eliminate the observable error iteratively, thanks to the BEN property. Specifically, the output of the module Θ (i.e., compressed sensing circuitry) is re-projected by the system matrix A, and then the estimated data may be compared with the measured data. The difference is the data residual due to the observable error component. To suppress this error component, the reconstruction network Φ may be used to reconstruct an incremental image and update the current image with the module Θ (i.e., compressed sensing circuitry). In this correction step, the desirable incremental image is the new ground truth image, and the BEN property holds to make this step a contraction mapping; in other words, the associated new observable error is less than the previous observable error, thanks to the BEN property. Repeating this process many times, the observable error component will diminish geometrically (the ratio less than 1), so that the ACID solution will simultaneously incorporate data-driven knowledge, sparsity preference, and measurement data consistency.

In operation, the ACID reconstruction network is configured to transform an original measurement (e.g., a sinogram or a k-space dataset) into an initial image. The initial image may reflect a relatively strong image prior knowledge extracted from big data (e.g., CT or Mill data). This initial image is subject to errors and instabilities. The current image may then be improved by a compressed sensing inspired sparsity promotion module to output a sparsified image. Based, at least in part, on this sparse image, measurement data may be estimated using a system model (e.g., analytic mapping, A). The estimated and measured data may then be compared to determine a residual data that reflect observable errors, indicating whether the current image needs correction. A residual may be configured by the same deep reconstruction network to produce an incremental image on the top of the current image to form an updated image. This updated image is again processed by the compressed sensing module. This iterative process may be repeated to improve the current image gradually.

Thus, ACID may be configured to overcome at least some instabilities of neural networks indicating that accurate and stable deep reconstruction is feasible. The ACID network is configured to combine a sparsity-oriented algorithm, a data-driven direct reconstruction network, and an iterative data fidelity enforcement. It may be appreciated that the converging behavior and solution characteristics of ACID have been analyzed under an assumption termed a bounded error norm, a special case of a Lipschitz continuity. The Lipschitz continuity, used in the convergence analysis, may practically be interpreted as a Bounded Error Norm (BEN) property and has been experimentally verified in our study. Additionally or alternatively, it is not necessary that the measurement matrix satisfy a compressed sensing condition such as the restricted isometry property. This means that a standard sparsity-promotion algorithm may not give a unique solution. In this case, ACID may outperform the sparsity-minimization reconstruction alone, because data-prior may help fill in a gap in deep reconstruction. Last but not the least, in addition to an accurate reconstruction performance, ACID has stability in the two related aspects: (a) ACID can stabilize an unstable deep reconstruction network (by putting it in the ACID framework), and (b) ACID as a whole is resilient against adversarial attacks.

Turning now to the DRONE embodiment, compared to ACID, there are at least four main differences between DRONE and ACID. First, in the DRONE network, the deep prior in the measurement data domain is taken into account through both a projection expander and residual data refinement module, which is beneficial to improve the reconstruction performance, especially for sparse-data CT. Second, the residual data network and the residual image network of DRONE are re-trained using an incremental training-testing strategy, which can effectively avoid overfitting. Third, the predicted data and images are considered in the kernel awareness module simultaneously to further refine the

sparse-data CT reconstruction. Finally, deep priors for data and images are utilized only once in DRONE, instead of many times in ACID.

In one nonlimiting example, a classical analytic reconstruction algorithm (e.g., filtered back projection (FBP)) may be used for relatively fast reconstruction. It is contemplated that the image quality may be improved by replacing FBP with an iterative algorithm, such as a simultaneous algebraic reconstruction technique (SART) or an algebraic reconstruction technique (ART). The computational cost may be increased so that it becomes difficult to be implemented in time-sensitive clinical applications. Compared with SART and ART, FBP may be preferred for its efficiency and robustness. It may be appreciated that four network modules are trained for DRONE. It is contemplated that a weakly supervised learning may be utilized to relax a requirement for labeled big data.

Regarding regularization, a total variation (TV) method may be implemented in the awareness module (i.e., compressed sensing circuitry). Other advanced sparsity priors may be used, such as dictionary learning. Advanced priors may improve the image quality but they are computationally demanding. In practice, reconstruction performance and computational overhead should be balanced.

Although the deep learning-based tomographic reconstruction methods have achieved great successes in the past several years, the generalizability and robustness of trained networks is still an open problem in clinical applications. For example, the application of a network trained on data from one type of scanners to data from another type of scanner remains a challenge due to different imaging parameters and various technical factors. A feasible strategy for improving the robustness and generalization of deep tomographic reconstruction is to combine traditional reconstruction methods and deep networks, i.e., a hybrid image reconstruction system. A DRONE network is one example of this approach.

FIG. **1** illustrates a functional block diagram of a hybrid image reconstruction system **102** consistent with several embodiments of the present disclosure. System **102** is configured to receive an input data set, i.e., input data **104**, that corresponds to measured data, and to provide refined image data **106** as output. System **102** includes a deep learning stage **110** and a compressed sensing stage **112**. As used herein, a deep learning stage is configured to include at least one artificial neural network. The deep learning stage **110** is configured to receive the measured input data **104**, to operate on the input data to determine a deep learning stage output, and to provide intermediate data **114** to the compressed sensing stage **112**. The intermediate data **114** corresponds to a deep learning stage output.

Input data **104** corresponds to measured input data and may include tomographic data (e.g., projection data, sinogram data, k-space data, and/or raw data) from an imaging scanner. For example, the input data may correspond to projection data from a computed tomography (CT) scanner. In another example, the input data **104** may correspond to k-space data from a magnetic resonance imaging (MM) apparatus. In another example, the input data **104** may correspond to raw data from another imaging technology (e.g., positron emission tomography (PET), ultrasound, single photon emission computed tomography (SPECT), etc.). In some embodiments, the projection data may be sparse. In one nonlimiting example, low dose CT or C-arm CT scans may result in sparse input data.

Compressed sensing stage **112** is configured to receive the deep learning stage output, i.e., the intermediate data **114**, and to provide refined image data as output image data **106**. The refined image data corresponds to the input data set. In some embodiments, compressed sensing stage **112** may be configured to receive input data **104**. In some embodiments, an intermediate output **116** from compressed sensing stage **112** may be provided to deep learning stage **110**, as will be described in more detail below. Deep learning stage **110** may include deep learning refinement circuitry **120**. Deep learning refinement circuitry may include mapping circuitry **124**. Mapping circuitry **124** may include an analytic forward projection model and is configured to link a tomographic data domain and the image domain. In other words, mapping circuitry **124** is configured to provide image-to-data mapping (where "data" corresponds to tomographic data).

Compressed sensing stage **112** may include compressed sensing refinement circuitry **122**.

System **102** further includes a processor circuitry **132**, a memory circuitry **134**, an input/output (I/O) circuitry **136**, and a user interface (UI) **138**. Processor circuitry **132** may be configured to perform one or more operations of hybrid image reconstruction system **102** (e.g., deep learning stage **110**, and/or compressed sensing stage **112**). Memory circuitry **134** may include one or more types of memory, as described herein. Memory circuitry **134** may be configured to store information and/or data associated with deep learning stage **110**, compressed sensing stage **112**, and/or processor circuitry **132**, I/O circuitry **136**, and/or UI **138**. UI **138** may include a user input device (e.g., keyboard, keypad, mouse, touchpad, touch sensitive display, a microphone, etc.) and a user output device (e.g., a display, a loudspeaker, etc.).

In operation, hybrid image reconstruction system **102** may be configured to receive input data **104**, to apply both deep learning and compressed sensing techniques and to provide refined reconstructed image data as output while maintaining stability.

FIG. **2** illustrates a functional block diagram of one embodiment of a hybrid image reconstruction system **202** according to the present disclosure. System **202** is one example of hybrid image reconstruction system **102** of FIG. **1**. System **202** may be considered as an analytic compressive iterative deep framework ("ACID"). System **202** includes a deep learning stage **210** and a compressed sensing stage **212**. The deep learning stage **210** is configured to receive input data, and the compressed sensing stage **212** is configured to provide refined image data as output. The deep learning stage **210** includes initial reconstruction network circuitry **224** and may include deep learning refinement circuitry **220**. The compressed sensing stage **212** includes initial compressed sensing circuitry **226** and may include compressed sensing refinement circuitry **222**. Thus, deep learning stage **210** is one example of deep learning stage **110** of FIG. **1** and refinement circuitry **220** is one example of deep learning refinement circuitry **120**. Similarly, compressed sensing stage **212** is one example of compressed sensing stage **112** and refinement circuitry **222** is one example of compressed sensing refinement circuitry **122**.

Hybrid image reconstruction system **202** includes one or more refinement stages **218-1**, . . . , **218**-N. Each refinement stage **218-1**, . . . , **218**-N may include at least a portion of elements of deep learning refinement circuitry **220** and at least a portion of elements of compressed sensing refinement circuitry **222**. In other words, at least a portion of the deep learning stage refinement circuitry **220** and at least a portion of the compressed sensing stage refinement circuitry **222** correspond to a refinement stage.

A first refinement stage **218-1** includes mapping circuitry **228-1**, a residual reconstruction network circuitry **230-1**, a first summer (i.e., summing junction) **232-1**, a second summer **234-1**, and a compressed sensing circuitry **236-1**. Mapping circuitry **228-1**, residual reconstruction network circuitry **230-1**, the first summer **232-1**, and the second summer **234-1** are elements of deep learning refinement circuitry **220** and the compressed sensing circuitry **236-1** is an element of compressed sensing refinement circuitry **222**. An N^{th} refinement stage **218**-N includes mapping circuitry **228**-N, a residual reconstruction network circuitry **230**-N, a first summer **232**-N, a second summer **234**-N, and a compressed sensing circuitry **236**-N. Mapping circuitry **228**-N, residual reconstruction network circuitry **230**-N, the first summer **232**-N, and the second summer **234**-N are elements of deep learning refinement circuitry **220** and the compressed sensing circuitry **236**-N is an element of compressed sensing refinement circuitry **222**.

Each refinement stage **218-1**, . . . , **218**-N is configured to receive input data **104** (i.e., projection data) and to provide a respective refined image data **206-1**, . . . , **206**-N, as output. Each refinement stage **218-1**, . . . , **218**-N is further configured to receive a prior output image. Each refinement stage **218-1**, . . . , **218**-N may correspond to one iteration of refinement operations. Each refinement stage **218-1**, . . . , **218**-N is configured to provide incremental output image quality improvement and the hybrid image reconstruction system **202** may thus be configured to provide a gradual output image quality improvement. A system architecture of hybrid image reconstruction system **202**, that includes a plurality of refinement stages **218-1**, . . . , **218**-N, may thus correspond to an unrolled network architecture.

Initial reconstruction network circuitry **224**, and residual reconstruction network circuitry **230-1**, . . . , **230**-N correspond to deep learning neural networks. An initial compressed sensing circuitry **226**, and compressed sensing circuitry **236-1**, . . . , **236**-N are configured to implement compressed sensing based regularization. Input to initial reconstruction network circuitry **224** is input data, e.g., tomographic data, as described herein. Initial reconstruction network circuitry **224** is configured to reconstruct an initial image, i.e., initial image data **225**, and to provide the initial image data **225** (i.e., intermediate image data) to initial compressed sensing circuitry **226**. Initial compressed sensing circuitry **226** is configured to regularize the initial image data **225** and to provide as output refined image data **227**, corresponding to refined image data **106** of FIG. **1**. Output from initial compressed sensing circuitry **227** may be provided to a first refinement stage **218-1**, as described herein. Output from initial compressed sensing circuitry **227** may be provided as an initial image data **206-0** output from hybrid tomographic reconstruction system **202**.

In some embodiments, system **202** may be configured to refine the initial estimated image data **227** based, at least in part, on the input data **104** and corresponding residual data. Each refinement stage may be configured to refine a prior refined image data. For example, the first refinement stage **218-1** may be configured to refine the initial estimated image data **227** received from initial compressed sensing circuitry **226**. Mapping circuitry **228-1** may thus be configured to perform analytic mapping based, at least in part, on a system matrix, A. In an embodiment, the analytic mapping corresponds to a forward projection of refined image data **227** to corresponding estimated input data **229-1**, e.g., estimated tomographic data. The first summer **232-1** is then configured to determine a difference between the input data **104** and the estimated input data **229-1** and a corresponding residual **233-1** may then be provided the first residual reconstruction network circuitry **230-1**. The residual reconstruction network circuitry **230-1** may also correspond to a deep learning neural network. The residual reconstruction network circuitry **230-1** is configured to reconstruct a residual image **231-1**. The second summer **234-1** is configured to receive the reconstructed residual image **231-1** and the initial estimated image data **227**, to combine the images and provide a second summer output corresponding to combine the image data **235-1** to compressed sensing circuitry **236-1**. Compressed sensing circuitry **236-1** may then be configured to regularize the combined image data **235-1** yield a refined estimated output image corresponding to refined image data **206-1**.

Each refinement stage **218-1**, . . . , **218**-N may thus be configured to receive a prior refined image data from a prior compressed sensing circuitry. Each refinement stage **218-218**-N may be further configured to receive the input data **104**, and to generate an refined image data output, as described herein. The refined image data output (i.e., refined image data **206**-N) of a final refinement stage **218**-N may then correspond to refined image data **106** of FIG. **1**, i.e., the refined output image data of hybrid image reconstruction system **202**, corresponding to input data **104**.

Operation of hybrid image reconstruction system **202**, i.e., ACID, is described in Table 1: Pseudocode of ACID workflow. In the Table 1, $p^{(0)}$ corresponds to input data **104**, neural network Φ corresponds to reconstruction network circuitry **224**, **230-1**, . . . , **230**-N, and system matrix A corresponds to mapping circuitry **228-1**, . . . , **228**-N. Equation 1 corresponds to residual data, e.g., residual **233-1** that is output from summer **232-1**, and $f^{(k)}$ corresponds to image data of a k^{th} iteration, that is normalized, updated according to Equation 2 and then denormalized.

TABLE 1

Pseudocode of the ACID workflow.

Input: Data $p^{(0)}$, neural network Φ, system matrix A, maximum number of iterations auxiliary parameters ξ, λ, $\mu = 0$, and $k = 1$;

1. If $k<K+1$ do
2. if $k=1$ do
3. Computing $\Phi(p^{(0)})$;
4. Normalizing the $\Phi(p^{(0)})$;
5. Updating $b^{(1)}$ using Eq. (2) where the normalized $\Phi(p^{(0)})$ is treated as the input;
6. Updating $f^{(1)}$ by de-normalizing $b^{(1)}$;
7. else do

TABLE 1-continued

Pseudocode of the ACID workflow.
8. Computing residual data using $p^{(k+1)} = \frac{\lambda(p^{(0)} - Af^{(k)})}{1+\lambda+\mu}$;
9. Normalizing the residual data $p^{(k+1)}$ into the input range of neural network;
10. Inputting the normalized data into the neural network Φ and obtaining $\Phi(p^{(k+1)})$;
11. De-normalizing $\Phi(p^{(k+1)})$;
12. Normalizing $f^{(k)} + \frac{1+\mu\rho}{\lambda\rho}\Phi(p^{(k+1)})$
13. Updating $b^{(k+1)}$ utilizing Eq. (2);
14. Updating $f^{(k+1)}$ by de-normalizing $b^{(k+1)}$;
15. end
16. end
17. return $f^{(K)}$
Output: Reconstructed image $f^{(K)}$

$$p^{(k+1)} = \frac{\lambda(p^{(0)} - Af^{(k)})}{1+\lambda+\mu} \quad (1)$$

$$f^{(k+1)} = H^{*}S_{\frac{\xi}{\lambda\rho}}\left(H\left(f^{(k)} + \frac{1+\mu\rho}{\lambda\rho}\Phi(p^{(k+1)})\right)\right) \quad (2)$$

Thus, operation of the ACID system **202** may correspond to an iterative framework, as indicated in Table 1. Given input data $p^{(0)}$, a neural network Φ and a system matrix A. A stopping condition, i.e., the maximum number of iterations K, may be specified. Parameters ζ, λ and μ are configured to control the iterative process and the regularization strength may then be specified and/or determined empirically. In one nonlimiting example, the parameter μ may be set to 0.

When k=1, $\Phi(p^{(0)})$ may be computed and then normalized. The goal of the normalization operator is to facilitate the adjustment of the regularization parameters for different applications. Then, $b^{(1)}$ may then be updated according to Eq. (2). Next, $f^{(1)}$ may be updated by de-normalizing $b^{(1)}$. When $1<k<K+1$, the residual data may be determined according to Eq. (1). Since the residual data may not be in the dynamic range of the original data, the residual data may be normalized into the original range to support efficient operation of the neural network (Line #9 in Table 1). After the neural network (i.e., reconstruction network circuitry) predicts a residual image, the de-normalization operator may be applied on the prediction to provide consistency of the reconstruction results.

$$f^{(k)} + \frac{1+\mu\rho}{\lambda\rho}\Phi(p^{(k+1)})$$

may then be normalized and provided to the compressed sensing-based regularization module (i.e., compressed sensing circuitry) to encourage image sparsity. The updated image $f^{(k+1)}$ (i.e. refined image data **106**) may then be obtained after the de-normalization.

Thus, the ACID architecture (hybrid image reconstruction system **202**) for stabilizing deep tomographic image reconstruction may include deep reconstruction, compressed sensing-based sparsity promotion, analytic mapping and iterative refinement. $p^{(0)}$ corresponds to original tomographic data (i.e., input data), and $p^{(K_{ACID})}$, $k_{ACID}=1, 2, 3, \ldots, K_{ACID}$, represents an estimated residual dataset in the k_{ACID}^{th} iteration between $p^{(0)}$ and the currently reconstructed counterpart. $\Phi(p^{(K_{ACID})})$ is an output of the deep reconstruction module, and $f^{(K_{ACID})}$ represents the image after compressed sensing-based regularization.

FIG. **3** illustrates a functional block diagram of another embodiment of a hybrid image reconstruction system **302** according to the present disclosure. System **302** is another example of hybrid image reconstruction system **102** of FIG. **1**. System **302** may be considered as a dual-domain residual-based optimization network ("DRONE"). System **302** includes a deep learning stage **310** and a compressed sensing circuitry **312**. The deep learning stage **310** is configured to receive input data (γ), and the compressed sensing circuitry **312** is configured to provide image data as output. The input data may be sparse, as described herein. The deep learning stage **310** includes initial reconstruction network circuitry **322** and refinement circuitry **320**. The initial reconstruction circuitry **322** corresponds to an embedding module, the refinement circuitry **320** corresponds to a refinement module and compressed sensing circuitry **312** corresponds to an awareness module, as described herein. Deep learning stage **310** is one example of deep learning stage **110** and compressed sensing circuitry **312** is one example of compressed sensing stage **112** of FIG. **1**.

The initial reconstruction circuitry **322** includes a projection network circuitry **324**, a first reconstruction circuitry **326-1**, and an image domain network circuitry **328**. The projection network circuitry **324** and the image domain network circuitry **328** may both correspond to deep learning neural networks. The refinement circuitry **320** includes a mapping circuitry **330**, a first summer **332-1**, a second summer **332-2**, a residual data network circuitry **334**, a second reconstruction circuitry **326-2**, an image residual network circuitry **336**, and a third summer **332-3**. The residual data network circuitry **334**, and the image residual network circuitry **336** may both correspond to deep learning neural networks. It may be appreciated that the projection network circuitry **324** and the residual data network circuitry **334** may be configured to operate in the input data domain, e.g., tomographic data domain. Similarly, the image domain network circuitry **328** and the image residual network circuitry **336** may be configured to operate in the image data domain.

The reconstruction circuitry **326-1**, **326-2** are configured to reconstruct image domain data from input domain data. The mapping circuitry **330** is configured to generate input domain (i.e., projection domain) data from image domain data. The mapping circuitry **330** may thus have a corresponding matrix, A_2, configured to map image domain data to the projection domain. The compressed sensing circuitry **312** is configured to receive input data, y, as well as processed input domain data (z^d) **343** and image domain data (f^d) **342** from deep learning stage **310**, as described herein.

In operation, the initial reconstruction circuitry **322** is configured to receive input data corresponding to a sparse data set, y. Projection network circuitry **324** is configured to extend the sparse data set y to a relatively high-dimensional estimated data set: estimated projection data set (z_1) **325**. As used herein, "estimated projection data set" corresponds to estimated measurements, thus, estimated measurements may be highly dimensional. It may be appreciated that an implicit interpolation operation may introduce errors. Projection network circuitry **324** may be configured to interpolate part or all of the projection data set. It may be appreciated that prediction errors in the projection domain may be greater when the data are extended to angular positions further away from the viewing angles physically used. In one nonlimiting example, 60 measured views may be extended to a dataset of 180 views forming a half-scan, which is sufficient for the awareness module (i.e., compressed sensing circuitry **312**) to generate relatively high-quality images. However, this disclosure is not limited in this regard. Reconstruction circuitry **326-1** may then be configured to reconstruct the estimated projection data set **325** into a corresponding raw image using, for example, FBP reconstruction (Δ_2^+). Image domain network circuitry **328** may then be configured to post-process the FBP reconstruction output from reconstruction circuitry **326-1** into an estimated image data set **329** corresponding to improved image f'. The image domain network circuitry **328** may thus correspond to an image domain neural network.

The operations of initial reconstruction circuitry **322** may be described by Eq. (3) as:

$$f'=\phi_{s_2}(A_2^+(\Phi_{s_1}(y))) \tag{3}$$

where y is the sparse input data set, Φ_{s_1} represents projection network circuitry **324** and S_1 represents the parameters of projection network circuitry **324**, A_2^+ represents filtered back projection (FBP) reconstruction operations of reconstruction circuitry **326-1**, ϕ_{s_2} represents image domain network circuitry **328** and S_2 represents the parameters of image domain network circuitry **328**, and f' is the estimated image data set **329**.

In an embodiment, projection network circuitry **324** may be implemented as an encode-decode network. For example, the encode-decode network may be related to a U-net and may include shortcut connections. Thus, example projection network circuitry **324** may be configured to extract an intrinsic latent code in the data domain. Continuing with this example, mean squared error (MSE) between labels and predictions may be employed as the loss function, during training. As the generator, an encode-decode architecture is based on U-net with shortcuts to produce images as faithfully as possible, and then the discriminator is trained on the generated images and corresponding labels. Projection network circuitry **324** may thus be trained on labeled data, which is then used for data extension to facilitate reconstruction of image features. It may be appreciated that the data expanded from sparse views may be embedded in a higher-dimensional measurement space defined by the trained projection network circuitry **324**. In the training process, the original data may be expanded via nearest neighbor interpolation, and the interpolated data may then be refined by projection network circuitry **324**, subject to the constraint that at the locations of the original data the original input will be kept as output to ensure the consistency.

Image reconstruction may be implemented using the image domain network circuitry **328** of initial reconstruction circuitry **322**. Image domain network circuitry **328** may be trained on paired FBP images. In one nonlimiting example, a generative adversarial network with the Wasserstein distance (WGAN) as the discrepancy measure between distributions may avoid over-smoothed edges and/or missing details and support recovery of textures and/or signatures. In an embodiment, image domain network circuitry **328** may include a generative adversarial network (GAN) with parameters ϕ_{s_2}, and configured to remove the image artifacts. The GAN includes a generator ("G") and a discriminator ("D") and may utilize the Wasserstein distance as the discrepancy measure between distributions. Image domain network circuitry **328** may thus correspond to a WGAN. During WGAN training, D and G may be optimized by mini-maximizing the following objective function:

$$\min_G \max_D (L_{MSE}(u, G(t)) + \lambda_{wgan} \cdot L_{WGAN}(D, G)), \tag{4a}$$

$$L_{WGAN}(G, D) = \left\{ \begin{matrix} -E_u[D(u)] + E_t[D(G(t))] + \\ \eta E[(\nabla_{\hat{u}} D(\hat{u})_2 - 1)^2] \end{matrix} \right\}. \tag{4b}$$

It may be appreciated that the first two terms on the right side of Eq. (4b) are configured to estimate the Wasserstein distance, the last term is the gradient penalty for regularization, $\hat{u}$ may be uniformly sampled along straight lines connecting pairs of generated and actual samples, t represents corrupted images reconstructed using FBP, u is the corresponding label, and η is a constant for weighting parameter. In one nonlimiting example, η may be equal to ten. However, this disclosure is not limited in this regard. As is known, in a GAN, networks D and G are trained alternatively by fixing one and updating the other.

Within the GAN framework, a neural network having an encode-decode architecture based on U-net with shortcuts may be treated as a generator configured to produce images as faithfully as possible. The generated images and corresponding labels are treated as input to the discriminator. Thus, the image domain network circuitry **328** may be configured to remove sparse artifacts and to enhance image quality, via, for example, noise reduction. The discriminator discriminates between the output and label, and it informs the generator to improve image fidelity and structures.

Refinement circuitry **320** is configured to receive the estimated projection data set **325** (z'_1) and the estimated image data set **329** (f') from the initial reconstruction circuitry **322**, and to provide as output the updated data-image pair (z^d, f^d). It may be appreciated that because interpolation in the projection domain may introduce errors, the initial reconstruction circuitry (i.e., embedding module) **322** may produce relatively more errors when, for example, relatively more projections are estimated over a wider angular range. On the other hand, a relatively limited number of views may compromise performance in the image domain. In an embodiment, refinement circuitry **320** and compressed sensing circuitry **312** may be configured to solve this issue by

keeping a balance between extending the number of views and refining the subsequent results iteratively.

Mapping circuitry **330** is configured to receive the estimated image data set **329** (f') and to map image domain data to the projection domain, producing corresponding projection data set **331** (z'_1) that corresponds to A_2f'. Summer **332-1** is configured to subtract z'_1 from the estimated projection data set, z_1, to yield residual data input **333**, that is input to residual data network circuitry **334**.

Similar to the initial reconstruction circuitry **322**, refinement circuitry **320** includes two network circuitries: residual data network circuitry **334** and image residual network circuitry **336**. There may be discrepancies between the outputs, $\{z_1, f'\}$, of the initial reconstruction circuitry **322** and corresponding ground truths, $\{z_0, f_0\}$. The re-sampled residual data from estimated image data set **329** (f'), i.e., residual data input **333** may be expressed as: z_1-A_2f'. In an embodiment, residual data network circuitry **334** may be trained to Φ_{s_3} to handle residual data, with the MSE between labels and predictions as loss function. Φ_{s_3} may thus correspond to parameters of the residual data network circuitry **334**. The estimated data residual z_2 of the refinement circuitry **320** may then be expressed as:

$$z_2=\Phi_{s3}(z_1-A_2f'). \tag{5}$$

In addition or alternatively to the data difference computed by the trained data residual network according to Eq. (5), there may be an image difference between the output of the initial reconstruction circuitry **322** and the ground truth. Image residual network circuitry **336** may be trained and may have parameters ϕ_{s_4}. The training may be configured to refine image details by minimizing the MSE between labels and predictions. In one nonlimiting example, training may include data from different patients in training each of the four networks in the DRONE architecture **302** configured to reduce the overfitting risk. A residual image, corresponding to an output of image residual network circuitry may then be defined as:

$$f''=\phi_{s4}(A_2^+(z_2)) \tag{6}$$

In an embodiment, similar to the projection network circuitry **324** in the initial reconstruction circuitry **322**, residual data network circuitry **334** may be implemented as an encode-decode network. Residual data network circuitry **334** may be implemented with a similar encode-decode architecture except for an interpolation layer. It may be appreciated that Φ_{s_3} may generally converge relatively quickly. In other words, details of residual data network circuitry **334** may be relatively easy to learn. Thus residual data network circuitry **334** may be trained with relatively less data.

The image residual network circuitry **336** and network parameters, ϕ_{s_4}, are configured to provide image accuracy. The image residual network circuitry **336** may thus include a discriminator network. A discriminator network may be configured to decrease quantitative scores. Thus, relatively high-dimensional data, z_1, and a corresponding image, f', may be improved simultaneously as:

$$z^d=z_2+A_2f' \tag{7}$$

and

$$f^d=f'+g'' \tag{8}$$

where $\{z^d, f^d\}$ corresponds to the updated data-image pair. It may be appreciated that the updated image pair exhibit an improvement over the input data. The updated data-image pair may then be provided to the compressed sensing circuitry for possible further improvement.

Compressed sensing circuitry **312** (i.e., awareness module) may be configured as an optimization with constraint(s). For example, regarding regularization, a total variation (TV) method may be implemented in compressed sensing circuitry **312**. In another example, other advanced sparsity priors may be used, such as dictionary learning. Advanced priors may improve the image quality but they are computationally demanding. In practice, reconstruction performance and computational overhead should be balanced.

As is known, sparse-view reconstruction is one example of a typical undetermined inverse problem, and there has not been a general solution that delivers good image quality if the number of views is relatively small, e.g., less than 100 views. Compressed sensing may provide a utility for, for example, sparse-data medical CT. In one nonlimiting example, a total variation minimization technique may be beneficial to image recovery with edge preservation. In an embodiment, a total difference for f may be defined as:

$$Wf = \sum_{n_h=2}^{N_H}\sum_{n_w=2}^{N_W}(|f(n_w,n_h)-f(n_w,n_h-1)|+|f(n_w,n_h)-f(n_w-1,n_h)|) \tag{9}$$

where the gradient magnitudes along an image border are set to zero.

The initialization and constraints play a role to reconstruct images from subsampled measurements because they can narrow the feasible region in the solution space. This idea leads to a combination of the deep learning-enabled data-image priors $\{z^d, f^d\}$ with the CS framework as:

$$\min_f\left\{\frac{1}{2}\|y-A_1f\|_F^2+\frac{\lambda_1}{2}\|z^d-A_2f\|_F^2+\frac{\lambda_2}{2}Wf+\frac{\lambda_3}{2}W(f-f^d)\right\} \tag{10}$$

where λ_1 is a hyper-parameter and $\lambda_1\geq 0$ is configured to balance two data fidelity terms: $\frac{1}{2}\|y-A_1f\|_F^2$ and $\frac{1}{2}\|z^d-A_2f\|_F^2$. A_1 represents the system matrix that projects to low-dimension data domain. If the error of z^d is small, a greater value for λ_1 should be selected. λ_2 and λ_3 are hyper-parameters for regularizations, which are used to balance the data fidelity terms and regularization priors. In Eq. (10), the data-image priors from the neural networks are considered, because the L_1-norm optimization is utilized. Since it is difficult to obtain a solution directly, two vectors v_1 and v_2 may be introduced to replace fin Wf and $(f-f^d)$, respectively. Then, Eq. (10) becomes a constrained optimization problem:

$$\min_{f,v_1,v_2}\left\{\frac{1}{2}\|y-A_1f\|_F^2+\frac{\lambda_2}{2}Wv_1+\frac{\lambda_1}{2}\|z^d-A_2f\|_F^2+\frac{\lambda_3}{2}Wv_2\right\},\ \text{s.t.},\quad f=v_1,\ f-f^d=v_2. \tag{11}$$

Eq. (11) may then be converted into the following unconstrained optimization problems under proper conditions:

$$\min_{\{f,v_1,v_2,f_1,f_2\}}\left\{\begin{array}{l}\frac{1}{2}\|y-A_1f\|_F^2+\frac{\lambda_1}{2}\|z^d-A_2f\|_F^2+\frac{\alpha_1}{2}\|f-v_1-f_1\|_F^2+\\ \frac{\lambda_2}{2}Wv_1+\frac{\lambda_3}{2}Wv_2+\frac{\alpha_2}{2}\|f-f^d-v_2-f_2\|_F^2\end{array}\right\} \quad (12)$$

where f_1 and f_2 are error vectors, and $\alpha_1 \leq 0$ and $\alpha_2 \geq 0$ are the coupling coefficients. Noting that there are five variables in Eq. (12), Eq. (12) can be divided into the following five sub-problems:

$$\min_f\left\{\begin{array}{l}\frac{1}{2}\|y-A_1f\|_F^2+\frac{\alpha_1}{2}\|f-v_1^{(k)}-f_1^{(k)}\|_F^2+\\ \frac{\lambda_1}{2}\|z^d-A_2f\|_F^2+\frac{\alpha_2}{2}\|f-f^d-v_2^{(k)}-f_2^{(k)}\|_F^2\end{array}\right\}, \quad (13)$$

$$\min_{v_1}\left\{\frac{\alpha_1}{2}\|f^{(k+1)}-v_1-f_1^{(k)}\|_F^2+\frac{\lambda_2}{2}Wv_1\right\}, \quad (14)$$

$$\min_{v_2}\left\{\frac{\alpha_2}{2}\|f^{(k+1)}-f^d-v_2-f_2^{(k)}\|_F^2+\frac{\lambda_3}{2}Wv_2\right\}, \quad (15)$$

$$f_1^{(k+1)}=f_1^{(k)}-\left(f^{(k+1)}-v_1^{(k+1)}\right), \quad (16)$$

$$f_2^{(k+1)}=f_2^{(k)}-\left(f^{(k+1)}-f^d-v_2^{(k+1)}\right), \quad (17)$$

where k denotes the index for the current iteration. Regarding the sub-problem Eq. (13), the minimizer is configured to satisfy the condition of the derivative equaling zero, i.e.,

$$A_1^T(A_1f-y)+\alpha_1(f-v_1^{(k)}-f_1^{(k)})+\lambda_1A_2^T(A_2f-z^d)+\alpha_2(f-f^d-v_2^{(k)}-f_2^{(k)})=0. \quad (18)$$

f may then be updated as

$$f^{(k+1)}=f^{(k)}-(A_1^TA_1+\lambda_1A_2^TA_2+\alpha_1+\alpha_2)^{-1}\{\lambda_1A_2^T(A_2f^{(k)}-z^d)+A_1^T(A_1f^{(k)}-y)+\alpha_1(f^{(k)}-v_1^{(k)}-f_1^{(k)})+\alpha_2(f^{(k)}-f^d-v_2^{(k)}-f_2^{(k)})\}, \quad (19)$$

where A_1^T and A_2^T can be computed using an ART, SART, or another classic algorithm. An analytic reconstruction method, i.e., A_1^T and A_2^T may be replaced with A_1^+ and A_2^+, and A_1^+ and A_2^+, and $A_1^TA_1$ and $A_2^TA_2$ may be treated as identical transforms. FBP may be employed for fast initial image reconstruction. The optimization of Eq. (14) corresponds to the total variation minimization problem. First $f(n_w, n_h)-f(n_w, n_h-1)$ and $f(n_w, n_h)-f(n_w-1, n_h)$ may be replaced with $d_1(n_w, n_h)$ and $d_2(n_w, n_h)$, and then Eq. (9) may be substituted into Eq. (14) to obtain

$$\min_{\{v_1,d_1,d_2\}}\left\{\begin{array}{l}\frac{1}{2}\|f^{(k+1)}-v_1-f_1^{(k)}\|_F^2+\frac{\lambda_2}{2}\times\\ \sum_{n_h=2}^{N_H}\sum_{n_W=2}^{N_W}\left(\begin{array}{l}|d_1(n_w,n_h)|+|d_2(n_w,n_h)|+\\ \frac{\rho}{2}\|d_1(n_w,n_h)-(f(n_w,n_h)-f(n_w,n_h-1))\|_2^2+\\ \frac{\rho}{2}\|d_1(n_w,n_h)-(f(n_w,n_h)-f(n_w-1,n_h))\|_2^2\end{array}\right)\end{array}\right\}. \quad (20)$$

v_1 may be updated using, for example, a Chambolle Antonin method. Eq. (20) corresponds to a typical image recovery task using TV minimization, and three variables (i.e., d_1, d_2 and v_1) may be updated using the alternating minimization strategy. In one nonlimiting example, the TV minimization may be implemented by the denoise_tv_chambolle function in the scikit-image library. The maximum number of iterations may be set to 100, with the other parameters as per default except for the denoising weight. For example, the denoising weight for updating v_1 may be set as β_1, which may be optimized for specific applications. The solution to Eq. (15) for v_2 is the same for v_1, where the denoising weight is set to β_2 in a task-specific fashion.

Generally, this disclosure relates to a hybrid image reconstruction system. In some embodiments, the hybrid image reconstruction system includes a deep learning stage and a compressed sensing stage. The deep learning stage is configured to receive an input data set that includes measured tomographic data and to produce a deep learning stage output. The deep learning stage includes a mapping circuitry, and at least one artificial neural network. The mapping circuitry is configured to map image domain data to a tomographic data domain. The compressed sensing stage is configured to receive the deep learning stage output and to provide refined image data as output. In one embodiment, the hybrid image reconstruction system may correspond to an analytic compressive iterative deep framework ("ACID"). In another embodiment, the hybrid image reconstruction system may correspond to a dual-domain residual-based optimization network (DRONE). A deep reconstruction network may be stabilized in a hybrid model that combines deep learning and compressed sensing.

FIG. **4** is a flowchart **400** of example hybrid image reconstruction operations consistent with various embodiment of the present disclosure. In particular, the flowchart **400** illustrates producing refined image data for input data that includes tomographic data. The operations of flowchart **400** may be performed by, for example, hybrid image reconstruction system **102** (e.g., deep learning stage **110** and/or compressed sensing stage **112**) of FIG. **1** and/or hybrid image reconstruction system **202** (e.g., deep learning stage **210** and/or compressed sensing stage **212**) of FIG. **2**.

Operations of flowchart **400** may begin with receiving an input data set at operation **402**. The input data set may include tomographic data. An initial deep learning stage output may be produced at operation **404**. The deep learning stage may include at least one artificial neural network. Operation **406** may include producing an initial image data output. Operation **408** may include producing a refined deep learning stage output based, at least in part, on prior image output data. Operation **410** may include producing a refined image data output based, at least in part, on refined deep learning stage output. Operations **408** (producing a refined deep learning stage output based, at least in part, on prior image output data) and **410** (producing a refined image data output based, at least in part, on refined deep learning stage output) may be repeated at operation **412**. Repeating operations **408** and **410** is configured to provide iterative refinement of the output image data configured to provide gradual image quality improvement.

Thus, refined image data may be produced for input data that includes tomographic data.

FIG. **5** is a flowchart **500** of example hybrid image reconstruction operations consistent with various embodiment of the present disclosure. In particular, the flowchart **500** illustrates producing refined image data for input data that includes tomographic data. The operations of flowchart **500** may be performed by, for example, hybrid image reconstruction system **102** (e.g., deep learning stage **110** and/or compressed sensing stage **112**) of FIG. **1** and/or hybrid image reconstruction system **302** (e.g., deep learning stage **310** and/or compressed sensing circuitry **312**) of FIG. **3**.

Operations of flowchart **500** may begin with receiving an input data set at operation **502**. The input data set may

include tomographic data. A deep learning stage output may be produced at operation **504**. The deep learning stage may include at least one artificial neural network. Operation **506** may include receiving the deep learning stage output. For example, the deep learning stage output may be received by a compressed sensing stage. Refined image data may be provided as output at operation **508**.

Thus, refined image data may be produced for input data that includes tomographic data. As used in any embodiment herein, the term "logic" or "module" may refer to an app, software, firmware and/or circuitry configured to perform any of the aforementioned operations. Software may be embodied as a software package, code, instructions, instruction sets and/or data recorded on non-transitory computer readable storage medium. Firmware may be embodied as code, instructions or instruction sets and/or data that are hard-coded (e.g., nonvolatile) in memory devices.

"Circuitry", as used in any embodiment herein, may include, for example, singly or in any combination, hardwired circuitry, programmable circuitry such as computer processors including one or more individual instruction processing cores, state machine circuitry, and/or firmware that stores instructions executed by programmable circuitry. The logic or modules may, collectively or individually, be embodied as circuitry that forms part of a larger system, for example, an integrated circuit (IC), an application-specific integrated circuit (ASIC), a system on-chip (SoC), desktop computers, laptop computers, tablet computers, servers, smart phones, a field-programmable gate array (FPGA), a programmable logic device (PLD), a complex programmable logic device (CPLD), etc.

Processor circuitry **132** may include, but is not limited to, a single core processing unit, a multicore processor, a graphics processing unit, a microcontroller, an application-specific integrated circuit (ASIC), a field programmable gate array (FPGA), a programmable logic device (PLD), etc.

Memory circuitry **134** may include one or more of the following types of memory: semiconductor firmware memory, programmable memory, non-volatile memory, read only memory, electrically programmable memory, random access memory, flash memory, magnetic disk memory, and/or optical disk memory. Either additionally or alternatively memory **134** may include other and/or later-developed types of computer-readable memory.

Embodiments of the operations described herein may be implemented in a computer-readable storage device having stored thereon instructions that when executed by one or more processors perform the methods. The processor may include, for example, a processing unit and/or programmable circuitry. The storage device may include a machine readable storage device including any type of tangible, non-transitory storage device, for example, any type of disk including floppy disks, optical disks, compact disk read-only memories (CD-ROMs), compact disk rewritable (CD-RWs), and magneto-optical disks, semiconductor devices such as read-only memories (ROMs), random access memories (RAMs) such as dynamic and static RAMs, erasable programmable read-only memories (EPROMs), electrically erasable programmable read-only memories (EEPROMs), flash memories, magnetic or optical cards, or any type of storage devices suitable for storing electronic instructions.

What is claimed is:

1. A hybrid image reconstruction system, the system comprising:

a deep learning stage configured to receive an input data set comprising measured tomographic data and to produce a deep learning stage output, the deep learning stage comprising a mapping circuitry, and at least one artificial neural network, the mapping circuitry configured to map image domain data to a tomographic data domain; and

a compressed sensing stage configured to receive the deep learning stage output and to provide refined image data as output.

2. The system of claim **1**, wherein the deep learning stage comprises an initial reconstruction network circuitry, and a deep learning stage refinement circuitry comprising at least one mapping circuitry, and at least one residual reconstruction network circuitry, and

the compressed sensing stage comprises an initial compressed sensing circuitry, and a compressed sensing stage refinement circuitry comprising at least one refinement compressed sensing circuitry,

at least a portion of the deep learning stage refinement circuitry and at least a portion of the compressed sensing stage refinement circuitry corresponding to a refinement stage,

the initial reconstruction network circuitry configured to receive the input data set and to reconstruct a corresponding initial image data, and the initial compressed sensing circuitry configured to regularize the initial image data to yield an estimated image data,

each mapping circuitry configured to receive a prior compressed sensing circuitry image data output and to produce a respective corresponding projection data set, and

each residual reconstruction network circuitry configured to receive a respective residual projection data set corresponding to a difference between the input data set and the respective prior corresponding projection data set and to determine a respective corresponding residual image data, and

each refinement compressed sensing circuitry configured to receive a sum of a prior compressed sensing circuitry image data output and the respective corresponding residual image data and to produce a respective refined image data output.

3. The system of claim **2**, wherein a system architecture corresponds to an unrolled network architecture that comprises a plurality of refinement stages.

4. The system of claim **3**, wherein a respective refinement stage comprises a respective mapping circuitry, a respective residual reconstruction circuitry and a respective refinement compressed sensing circuitry.

5. The system of claim **2**, wherein each residual projection data set is normalized, and each residual image data is denormalized.

6. The system of claim **1**, wherein the deep learning stage comprises an initial reconstruction circuitry, and a refinement circuitry,

the initial reconstruction circuitry configured to receive the input data set, to determine an estimated projection data set based, at least in part, on the input data set, and to determine an refined image data set based, at least in part, on the estimated projection data set, and

the refinement circuitry configured to receive the estimated projection data set and the refined image domain data set, and to determine an updated data-image pair, the updated data-image pair corresponding to the deep learning stage output.

7. The system of claim **6**, wherein the initial reconstruction circuitry comprises a projection network circuitry, and an image domain network circuitry, and

the refinement circuitry comprises a residual data network circuitry, and an image residual network circuitry, each network circuitry corresponding to an artificial neural network configured to operate in a projection data domain or an image data domain.

8. The system of claim **6**, wherein the input data set is sparse and the estimated measurements are relatively highly dimensional.

9. The system of claim **7**, wherein the projection network circuitry and the image domain network circuitry each corresponds to a respective encode-decode network and the image domain network circuitry corresponds to a generative adversarial network (GAN).

10. The system of claim **1**, wherein the input data is selected from the group comprising computed tomography (CT), magnetic resonance imaging (MRI), positron emission tomography (PET), and single photon emission computed tomography (SPECT) tomographic data.

11. A method for hybrid image reconstruction, the method comprising:

receiving, by a deep learning stage, an input data set comprising measured tomographic data;

producing, by the deep learning stage, a deep learning stage output, the deep learning stage comprising a mapping circuitry, and at least one artificial neural network, the mapping circuitry configured to map image domain data to a tomographic data domain;

receiving, by a compressed sensing stage, the deep learning stage output; and

providing, by the compressed sensing stage, refined image data as output.

12. The method of claim **11**, wherein the deep learning stage comprises an initial reconstruction network circuitry, and a deep learning stage refinement circuitry comprising at least one mapping circuitry, and at least one residual reconstruction network circuitry, and the compressed sensing stage comprises an initial compressed sensing circuitry, and a compressed sensing stage refinement circuitry comprising at least one refinement compressed sensing circuitry, at least a portion of the deep learning stage refinement circuitry and at least a portion of the compressed sensing stage refinement circuitry corresponding to a refinement stage, and further comprising:

reconstructing, by the initial reconstruction network circuitry, a corresponding initial image data based, at least in part, on the input data set; and

regularizing, by the initial compressed sensing circuitry, the initial image data to yield an estimated image data;

producing, by each mapping circuitry, a respective corresponding projection data set based, at least in part on, a prior compressed sensing circuitry image data output;

producing, by each residual reconstruction network circuitry, a respective corresponding residual image data based, at least in part, on a respective residual projection data set corresponding to a difference between the input data set and the respective prior corresponding projection data set;

receiving, by each refinement compressed sensing circuitry, a sum of a prior compressed sensing circuitry image data output and the respective corresponding residual image data; and

producing, by each refinement compressed sensing circuitry, a respective refined image data output.

13. The method of claim **12**, wherein a system architecture corresponds to an unrolled network architecture that comprises a plurality of refinement stages.

14. The method of claim **13**, wherein a respective refinement stage comprises a respective mapping circuitry, a respective residual reconstruction circuitry and a respective refinement compressed sensing circuitry.

15. The method of claim **12**, wherein each residual projection data set is normalized and each residual image data is denormalized.

16. The method of claim **11**, wherein the deep learning stage comprises an initial reconstruction circuitry, and a refinement circuitry, and further comprising:

receiving, by the initial reconstruction circuitry, the input data set;

determining, by the initial reconstruction circuitry, an estimated projection data set based,

at least in part, on the input data set;

determining, by the initial reconstruction circuitry, an refined image data set based, at least in part, on the estimated projection data set;

receiving, by the refinement circuitry, the estimated projection data set and the refined image domain data set; and

determining, by the refinement circuitry, an updated data-image pair, the updated data image pair corresponding to the deep learning stage output.

17. The method of claim **16**, wherein the initial reconstruction circuitry comprises a projection network circuitry, and an image domain network circuitry, and

the refinement circuitry comprises a residual data network circuitry, and an image residual network circuitry, each network circuitry corresponding to an artificial neural network configured to operate in a projection data domain or an image data domain.

18. The method of claim **16**, wherein the input data set is sparse and the estimated measurements are relatively highly dimensional.

19. The method of claim **17**, wherein the projection network circuitry and the image domain network circuitry each corresponds to a respective encode-decode network and the image domain network circuitry corresponds to a generative adversarial network (GAN).

20. The method of claim **11**, wherein the input data is selected from the group comprising computed tomography (CT), magnetic resonance imaging (MRI), positron emission tomography (PET), and single photon emission computed tomography (SPECT) input data.

21. The system of claim **1**, wherein the compressed sensing stage implements a total variation method.

22. The system of claim **1**, wherein the compressed sensing stage implements a low-rank method.

23. The system of claim **1**, wherein the compressed sensing stage implements a dictionary learning method.

* * * * *